Experimental Verification and Analysis of AC-DC Converter with an Input Impedance Matching for Wireless Power Transfer Systems

Keisuke Kusaka, Jun-ichi Itoh
Nagaoka University of Technology
1603-1 Kamitomioka-machi
Nagaoka Niigata, JAPAN
Tel.: +81 / (258) – 47 – 9563.
Fax: +81 / (258) – 47 – 9563.
E-Mail: kusaka@stn.nagaokaut.ac.jp, itoh@vos.nagaokaut.ac.jp
URL: http://itohserver01.nagaokaut.ac.jp/itohlab/en/index.html

This work was supported by Japan Society for the Promotion of Science; Grant-in-Aid for Scientific Research (B), 2436016.

Keywords

« Wireless power transmission », « Power converters for EV », « High frequency power converter »

Abstract

This paper discusses the performance of an AC-DC converter which converts power from 13.56-MHz AC to DC in a receiving side of wireless power transfer systems. The wireless power transfer systems are required to operate in high-frequency such as 13.56 MHz in order to achieve a high power density of transmission coils. Thus the AC-DC converter in the receiving side is demanded to operate at high-frequency. In such high-frequency region, the reflected power occurs when the input impedance is not matched to the characteristic impedance of the transmission line. In other words, the input impedance of the AC-DC converter needs to have the same impedance to the characteristic impedance of the transmission line. In order to overcome the problem, the AC-DC converter with an input impedance matching is proposed in this paper.

The proposed AD-DC converter achieves the input impedance matching with a simple circuit configuration. It means that the converter can obtain sinusoidal input current and unity input power factor without a high-frequency switching except the diodes. In this paper, the impedance matching characteristics and the analysis of the operational modes of the proposed circuit are presented. The experimental results confirmed that the proposed converter enables a conversion from 13.56-MHz AC to DC with the sinusoidal input current. In this operation condition, the input impedance is $29.6 + j0.51\ \Omega$. Because the design value of the input impedance is $50 + j0\ \Omega$, there is a non-negligible error on the real part. This is attributed to the parasitic capacitances on the diodes. In order to solve this problem, an improved AC-DC converter is proposed newly. From experimental results, it achieves the input impedance of $52.7 - j0.02\ \Omega$. Besides, the reflection coefficient is suppressed by up to 94.5% compared with that of the conventional capacitor input-type diode bridge rectifier (CI-DBR).

I. Introduction

In recent years, wireless power transfer methods have been attracted in the community [1-2]. In particular, the wireless power transfer with magnetic resonance coupling (MRC) which is reported by A. Karalis et al. in 2007 is heavily studied [3-4]. The MRC shows better features compared with the conventional wireless power transfer methods such as an electromagnetic induction and a microwave transmission. First, the MRC allows a wireless power transfer in a middle-range transmission distance such as a few dozen of centimeters at high efficiency of over 90% [5]. Such high transmission efficiency cannot be achieved with an electromagnetic induction. On the other hand, the transmission efficiency of a microwave transmission is greater than the others. However, the conversion efficiency between microwaves from electrical power is mere 84.4% [6].

Second, the declination of the transmission efficiency caused by a position gap of the transmitting devices is relatively small. These advantages are featured by the characteristic constructions of the transmitting coils. The transmission efficiency at a resonance frequency is expressed by (1). It represents the transmission efficiency is determined by an only product of the quality factor of the transmitting coil Q and the coupling coefficient k. The transmitting coils have a high quality factor Q owing to the low parasitic resistance of the coils. The high quality factor allows an efficient wireless power transfer in a middle-range transmission distance even when the coupling coefficient is small [7-8].

$$\eta = \frac{1}{1 + 2/kQ} \tag{1}$$

Considering to apply the wireless power transfer with MRC into the battery chargers for electrical vehicles (EVs), the coils for the transmitting side and receiving side are planted on the ground in parking areas, and underneath of EVs, respectively. This technology brings convenience to users because users are not required to charge the battery with electrical cables [9].

In the wireless power transfer system with the MRC, the size of the transmitting coils depends on the transmitting frequency [10]. Thus, the wireless power transfer systems are expected to operate in high-frequency in order to achieve a high power density. Moreover, MRC should be operated in industrial scientific medical (ISM) band such as 13.56 MHz and 27.12 MHz because noise from the wireless power transfer systems is prohibited to influence the operation of neither the electronic devices nor the radio communication equipment.

On the receiving side of wireless power transfer systems, the AC-DC converter, which converts the power from 13.56 MHz to DC, is necessary. The previous studies have reported that the use of the diode bridge rectifier on the receiving side [11]. The diode bridge rectifier has a distorted input current and low input power factor. Furthermore a diode bridge rectifier is connected to a DC load, the input impedance of the diode bridge rectifier depends on a load on a DC side. In such high-frequency region, an impedance matching is very important in order to suppress the reflected power [12]. Eventually, the reflected power which is generated by the input impedance mismatching decreases the transmission efficiency [11]. Besides, the characteristic impedance of the transmission line such as a coaxial cable is set to 50 + j0 Ω. Although, the matching function is required in the AC-DC converter, a method of an input impedance matching for the AC-DC converters has not been reported.

This paper proposes and demonstrates an input impedance of the AC-DC converter which can be matched to the characteristic impedance of 50 + j0 Ω. First, the configuration of the proposed AC-DC converter is described. The AC-DC converter achieves the input impedance matching without high-frequency switching devices except the diodes. Then, the operation modes of the proposed converter are analyzed. In particular, the formulas for the input current are derived. Finally, the AC-DC converter is tested experimentally.

II. Proposed AC-DC Converter with Input Impedance Matching

2.1. Requirements for Input Impedance Matching

Generally, high-frequency circuits are constructed with an impedance matching in order to suppress reflected power [12]. The impedance matching can be described as; the output impedance of the power supply and the input impedance have equal impedances to the characteristic impedance of the transmission line. In particular, the characteristic impedance of a 50 Ω is used widely. For this reason, 50 Ω is used as the characteristic impedance and also the input impedance of the AC-DC converter in this paper. Besides, the input impedance of AC-DC converters with a battery as a load is required to match an input impedance regardless of the load conditions.

In general, the characteristic impedance of transmission lines, which is the reference value of the input impedance of the AC-DC converter, does not include an imaginary part. Thus, an input voltage and current of the AC-DC converter are required to fulfill the following requirements, where $\dot{Z}_{in}$ is the input impedance, $\dot{V}_{in}$ is the fundamental input voltage of the AC-DC converter, $\dot{I}_{in}$ is the fundamental input current and θ is the phase angle between the input voltage and the input current.

(a) $\left|\dot{Z}_{in}\right| = \left|\dot{V}_{in}\right| / \left|\dot{I}_{in}\right| = 50\,\Omega$

(b) Input power factor is 1 (cos $\theta = 1$)

In a low-frequency region, power factor correction (PFC) circuits with a PWM control are used widely [13]. The PFC circuits with a PWM can satisfy the above-mentioned conditions easily due to the input current control with the PWM in a low-frequency region. However, the switching frequency for the PWM requires higher frequency than an input frequency. Thus, it is difficult to operate the conventional PFC circuits when the input frequency is constrained in a high-frequency such as 13.56 MHz. In conclusion, an AC-DC converter with a simple circuit configuration which can achieve the input impedance matching is required on the receiving side of the wireless power transfer system.

2.2. Circuit configuration

Fig. 1 presents the circuit configuration of the proposed AC-DC converter. The proposed converter consists of the resonant-type rectifier which is reported by K. Matsui et al. [14] and the bidirectional boost chopper. The resonant-type rectifier achieves a PFC operation using a resonance between the inductor which is connected in series to the input terminal and the capacitors in parallel to the upper arm. The resonant-type rectifier has been demonstrated in a commercial frequency in [14]. However, this converter causes a low power density in the low-frequency operation because a bulky inductor and capacitors as resonance components are required. Additionally, the possibility of the input impedance matching is not discussed. In this paper, the resonant-type rectifier is operated at high-frequency. Furthermore the function of the input impedance matching is evaluated. The high-frequency operation improves the power density owing to the downsizing of the passive components.

In addition, Ref. [14] pointed out that the amplitude of the input current and the input power factor hinge upon a load condition when a resistance load is connected directly to the resonant-type rectifier. It means that the input impedance of the stand-alone resonant-type rectifier depends on the load conditions. In order to overcome this problem, the bidirectional boost chopper is connected at the output side of the resonant-type rectifier in Fig. 1. The bidirectional boost chopper is operated in purpose to fix the operating point which is decided by the rectifier output voltage v_{ch} of the resonant-type rectifier. The MOSFET S_1 is used for an initial charge of the C_4 instead of a diode because the input power factor closes to zero when the rectifier outputs voltage v_{ch} is around zero.

The control for the chopper circuit does not need a high dynamic response. Thus, the chopper circuit does not need either a high-speed or a high-frequency switching. Thus, the chopper may be operated at a low switching frequency such as 20 kHz. However, a switching frequency of 100 kHz is selected in this paper with the objective of the downsizing of the inductor L_2.

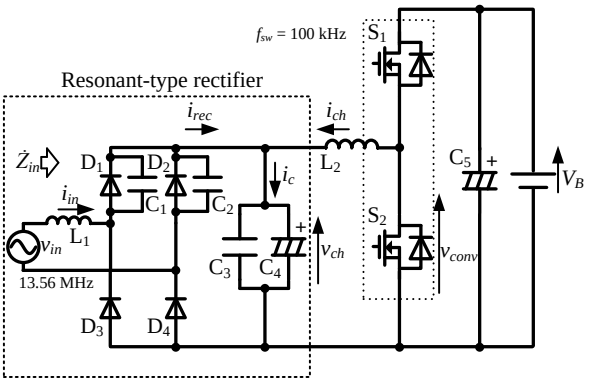

Fig. 1. The proposed AC-DC converter.

2.3. Control method of bidirectional boost chopper

Fig. 2 shows the control block diagram of the bidirectional boost chopper. The voltage control is composed by an automatic voltage regulator (AVR) with a PI control and an automatic current regulator (ACR) as an inner loop of the AVR, where the natural angular frequencies of the AVR and ACR are 400 rad/s and 4000 rad/s respectively. Note that T_{ic} and T_{iv} are the integral time of the ACR and AVR, respectively. The input impedance is determined by the relation among the voltage ratio α_V, the inductance L_1 and the capacitances C_1 and C_2 where the voltage ratio is the ratio of the rectifier output voltage v_{ch} to the input maximum voltage V_m. The voltage ratio should be stabilized in constant

in order to obtain the intended input impedance when the input power is constant. Thus, the voltage ratio is controlled through the rectifier output voltage control, where the reference value of the rectifier output voltage is obtained by (2).

$$v_{ch}^{*} = V_m \times \alpha_V^{*} \tag{2}$$

In the proposed circuit, a fast dynamic response of the bidirectional boost chopper is not necessary because the input maximum voltage is not changed fast. For this reason, an inexpensive general-purpose controller can be used. Note that, the capacitance C_3 is negligible in the AVR because the capacitance C_3 is enough smaller than C_4 in the control block diagram.

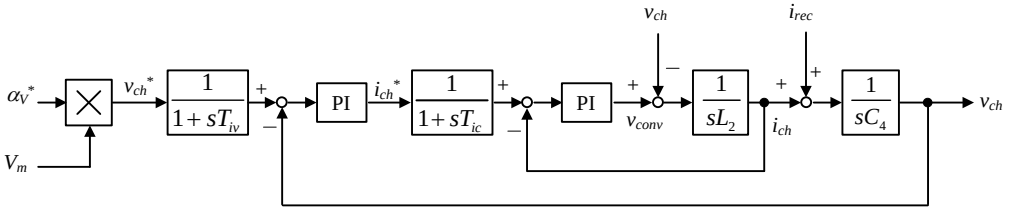

Fig. 2. The control block diagram for the proposed AC-DC converter.

III. Operation modes of the proposed AC-DC converter

Fig. 3 shows the operation modes of the proposed converter. Note that the bidirectional boost chopper with AVR is illustrated as an ideal DC voltage source.

Fig. 4 illustrates the simplified operation waveforms when the proposed converter is operated at the unity input power factor. In this chapter, the forward voltage drop of the diodes is ignored for simplicity. The circuit operations in each four operation are described in the following statements.

3.1. Operation mode I

Input current i_{in} flows through the inductor L_1, capacitors C_1 and C_2. The capacitors C_1 and C_2 are discharged and charged respectively by the input current. The input current in a mode I i_{in_I} is derived from a circuit equation as

$$i_{in\_I}(t) = \frac{\omega_{in}\omega_1^2 CV_m}{2\left(\omega_{in}^2 - \omega_1^2\right)}\left(\cos\omega_1 t - \cos\omega_{in} t\right) + \frac{\omega_1 C v_{ch}}{2}\sin\omega_1 t \tag{3},$$

where $C=C_1=C_2$, L is the inductance of the inductor L_1, V_m is the maximum input voltage, ω_{in} is the input angular frequency and ω_1 is the resonance angular frequency which is expressed as (4). Note that the resonance angular frequency is obtained as a series resonance of the inductance L and the two capacitances C.

$$\omega_1 = \frac{1}{\sqrt{LC/2}} \tag{4}$$

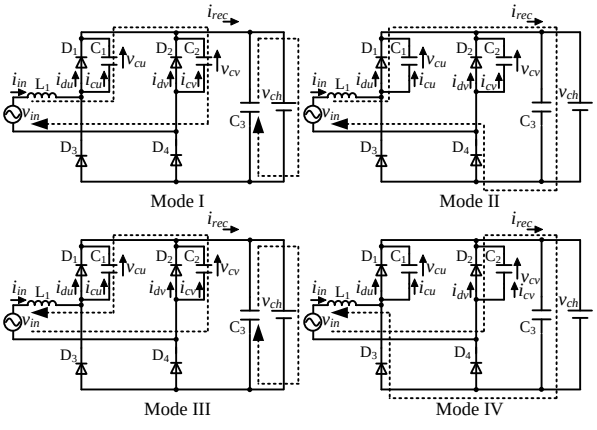

Fig. 3. Operation modes of the proposed circuit.

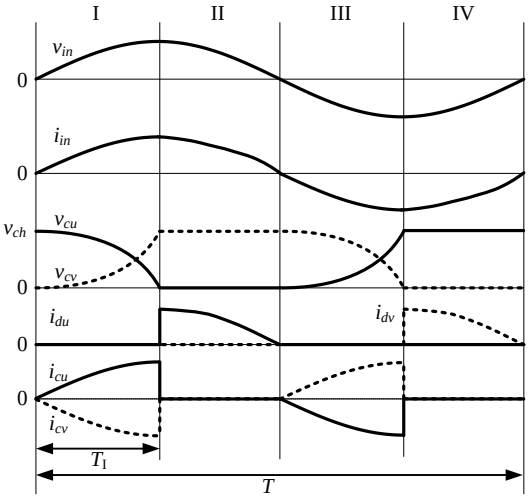

Fig. 4. Simplified waveforms of the proposed AC-DC converter.

From (3), the input current includes both the frequency components; resonance angular frequency ω_1 and input angular frequency ω_{in}. Thereby, the input current is not a complete sinusoidal waveform. The capacitor C_1, which had charged in operation mode III, is discharged by the input current. In contrast, the capacitor C_2 is charged gradually. After the capacitor voltage v_{cv} reaches to the DC voltage v_{ch}, the next operation mode will start.

Incidentally, the period of the operation mode I T_I is equal to the discharging time of the capacitor C_1. Thus, this period T_I can be derived from (5) with the numerical analytical approach.

$$\frac{v_{ch}}{2}\left(1+\cos\omega_1 T_I\right)+\frac{\omega_1 V_m}{2\left(\omega_{in}^2-\omega_1^2\right)}\left(\omega_1\sin\omega_{in}T_I-\omega_{in}\sin\omega_1 T_I\right)=0 \tag{5}$$

3.2. Operation mode II

The input current commutates to the diodes D_1 from the capacitor C_1 because the diodes D_1 and D_4 become a turn-on. The input current flows into the path that is formed by inductor L_1, diodes D_1 and D_4. In this mode, the smoothing capacitor is charged by the input current, which is expressed by

$$\begin{aligned} i_{in\_II}(t) = {} & i_{in\_II}\big|_{t=T_I}\cos\omega_2\left(t-T_I\right)-\frac{v_{ch}}{\omega_2 L}\sin\omega_2\left(t-T_I\right) \\ & +\frac{V_m\cos\omega_{in}T_I}{\left(\omega_{in}^2-\omega_2^2\right)L}\left\{\omega_{in}\cos\omega_2\left(t-T_I\right)-\omega_{in}\cos\omega_{in}\left(t-T_I\right)\right\} \\ & +\frac{V_m\sin\omega_{in}T_I}{\left(\omega_{in}^2-\omega_2^2\right)L}\left\{\omega_{in}\sin\omega_{in}\left(t-T_I\right)-\omega_2\sin\omega_2\left(t-T_I\right)\right\} \end{aligned} \tag{6},$$

where $i_{in\_II}(T_I)$ is the initial value of the input current which is also expressed as $i_{in\_I}(T_I)$, ω_2 is the resonance angular frequency which is expressed by (7). Also, the input current in the mode II is not a complete sinusoidal.

$$\omega_2=\frac{1}{\sqrt{LC_3}} \tag{7}.$$

Besides, (6) can be simplified as (8), when the resonance angular frequency ω_2 is enough small to be ignored. Generally, the capacitance C_4 has a large capacitance because it should compensate the voltage fluctuation which is caused by the bidirectional boost chopper.

$$i_{in\_II}(t)\approx i_{in\_II}\big|_{t=T_I}-\frac{v_{ch}}{L}\left(t-T_I\right)+\frac{V_m}{\omega_{in}L}\left(\cos\omega_{in}T_I-\cos\omega_{in}t\right) \tag{8}$$

Besides, the capacitor voltages v_{cu} and v_{cv} are not changed in this mode. The mode II continues until the input voltage polarity is changed from positive to negative.

3.3. Operation mode III

In this mode, the input current flows in the opposite direction to the mode I via C_2, C_1 and L_1. In this mode, the input current is expressed by $i_{in\_III}(t) = -i_{in\_I}(t-T/2)$ where T is the input period. The capacitors C_2 and C_1 are discharged and charged respectively by the input current. The mode III continues until the capacitor voltage v_{cu} reaches to the DC voltage v_{ch}. The period of the mode III is same to the one of mode II.

3.4. Operation mode IV

The input current commutates to the diodes D_2 and D_3 from the capacitors C_1 and C_2. The input current is expressed by $i_{in\_IV}(t) = -i_{in\_II}(t-T/2)$.

The amplitude of the input current and the input power factor are determined by the parameters that are used for the resonance; capacitors C_1, C_2 and inductor L_1 and voltage ratio α_V. Hence the intended input impedance of the AC-DC converter can be obtained by a designing these parameters properly. However, the design method is omitted in this paper because of space limitation.

IV. Simulation Results of the Proposed AC-DC Converter

In this chapter, the simulation result of the proposed AC-DC converter is shown. Table I presents the simulation conditions. In the simulation, the rated power is assumed as 1 kVA because the wireless power transmission systems are expected to apply to the EV charger.

Fig. 5 presents the simulation waveforms of the proposed AC-DC converter. It is confirmed that the rectifier output voltage v_{ch} and chopper current i_{ch} track to the each reference value. Thus, the bidirectional boost chopper is operated normally according to the PI control. Moreover, a sinusoidal input current and unity input power factor are achieved. In this simulation, the input impedance is calculated from the fundamental component of the input voltage and input current as 50 + j0.0 Ω with using (9), where V_{in_1st} is the fundamental component of the input voltage, I_{in_1st} is the fundamental component of the input current and θ is the phase angle between the input voltage and input current of the fundamental component.

$$\dot{Z}_{in} = \frac{|V_{in\_1st}|}{|I_{in\_1st}|}\cos\theta + j\frac{|V_{in\_1st}|}{|I_{in\_1st}|}\sin\theta \tag{9}$$

It means that the proposed converter is capable of the input impedance matching to the 50 + j0 Ω at a reflection coefficient of 0.0% which is defined by

$$\Gamma = \left|\frac{\dot{Z}_0 - \dot{Z}_{in}}{\dot{Z}_0 + \dot{Z}_{in}}\right| = \sqrt{\frac{P_R}{P_F}} \tag{10},$$

where $\dot{Z}_0$ is the characteristic impedance, P_F is supplied travelling power to the AC-DC converter, P_R is the reflected power which occurs at the input terminal of the AC-DC converter. Note that the reflection coefficient is used widely in a research field of high-frequency circuits to evaluate the circuit performance. The squared reflection coefficient means the ratio of reflected power to the traveling power. In this paper, the input impedance is matched to a 50 + j0 Ω because it is most common impedance, although the input impedance of the proposed circuit can be matched to other intended impedances.

Table I: Simulacion conditions.

Items		Value
Inductors	L_1	551 nH
	L_2	2.3 mH
Capacitors	C_1, C_2	138 pF
	C_3	940 nF
	C_4	440 μF
	C_5	220 μF

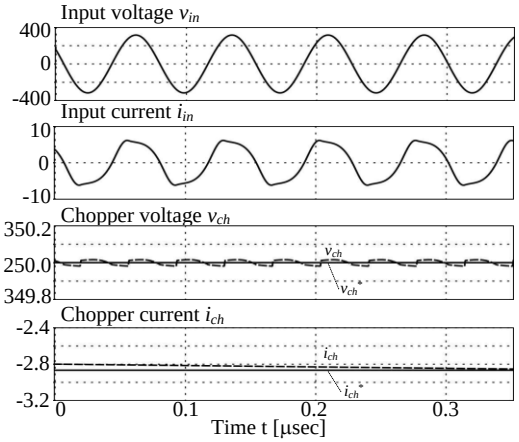

Fig. 5. Simulation result of the proposed AC-DC converter.

V. Experimental Results of the Proposed AC-DC Converter

Experimental verifications are shown in this chapter. Table II provides the circuit parameters for the experimental setup. Note that, the silicon carbide schottky barrier diodes (SiC-SBDs) are used in the rectifier because rectifying diodes are required to have a performance to rectify the 13.56–MHz AC. Besides, the design method of the resonance parameters, which affects the input impedance, is omitted in this paper due to the page limitation.

Table II: Parameters of the circuit components.

Items		Manufactures	Model number	Value
MOSFET	S_1, S_2	Vishay	IRFB11N50APBF	500 V, 11 A
Diode	D_1-D_4	Cree	C3D08060A	600 V, 8 A
Inductor	L_1	TDK	VLF10040T-1R5N8R9 (Remodeled)	950 nH
	L_2	-	-	2.3 mH
Capacitor	C_1, C_2	TDK	C3216C0G2J151JT	150 pF
	C_3	TDK	CKG57NX7R2J474M	470 nF (in parallel)
	C_4	nichicon	UPW2V221MRD	220 μF (in parallel)
	C_5	BHC Components	ALS30A221DB450	220 μF

5.1. Fundamental characteristics

Fig. 6 shows the experimental waveforms of the proposed AC-DC converter. It is clear that power conversion from 13.56 MHz to DC is achieved by the proposed converter with the sinusoidal input current and unity input power factor.

Fig. 7 presents the harmonics analysis results of the input voltage and current which is conducted in order to derive the input impedance from the experimental waveforms shown in Fig. 6. Note that, the probes; a differential probe (Tektronix, P5205) and a current probe (Tektronix, TCP312), which are used in these experiments provide a limitation to the frequency bandwidth at 100 MHz. For this reason, the harmonics components over 7^{th} are considered as reference values.

From the calculation with (9), the input impedance is calculated as $29.6 + j0.51\ \Omega$. The input impedance includes the non-negligible error on the real part. This is attributed to the parasitic capacitances of the SiC-SBDs. In the next subsection, the proposed circuit is improved in order to achieve intended input impedance.

Fig. 8 shows the reason of the error on the input impedance. In a high frequency region, the parasitic capacitances $C_{p1\text{-}4}$ of the diodes cannot be ignored. Especially, an effect of the parasitic capacitance increases when a reverse voltage of the diodes is high. The parasitic capacitances make a leakage current path during the operation modes I and III. Owing to the leakage current path, the input current is separated into the primary current path and the leakage current path. Thus the relation between the resonance capacitance C and the input impedance is different from the intended one. The combined capacitance on the upper arm is composed by the parasitic capacitances and additional capacitors. By contrast, the lower arm has only parasitic capacitances. Thus the current flowing through the upper and lower arms becomes unbalanced. It means that the design procedure of the

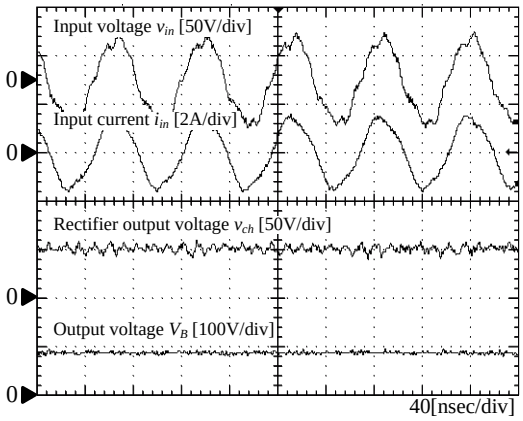

Fig. 6. Experimental waveforms of the proposed AC-DC converter.

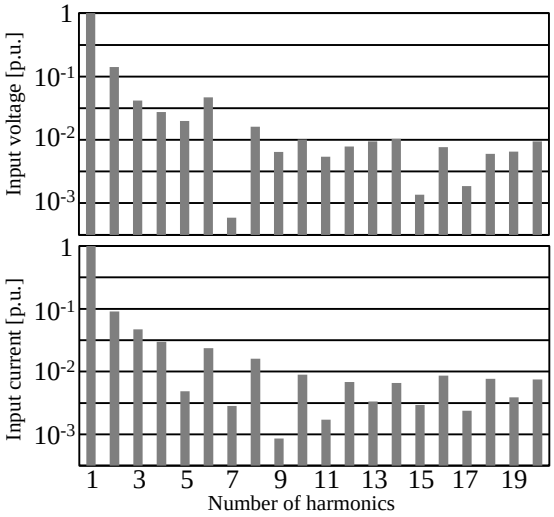

Fig. 7. Harmonics analysis of the input voltage and input current of the proposed AC-DC converter.

resonance capacitance C is complicated. In order to solve the above-mentioned problem, the improved AC-DC converter is newly proposed in the next subsection.

5.2. Improvement of impedance matching characteristics

Fig. 9 shows the improved AC-DC converter with an input impedance matching. Additionally, Table III provides the circuit parameters for the experimental setup with the improved AC-DC converter. The two resonance capacitors; C_6 and C_7 are added into the lower arm in the purpose of balancing the impedances between the upper arm and lower arm. Owing to these additional capacitors, the input impedance can be designed by considering the parasitic capacitances easily because the input current is shunted equally to the each arm in the mode I.

Fig. 10 presents the operation modes of the improved AC-DC converter. The operation modes of the improved AC-DC converter are similar to the one of the AC-DC converter without an improvement. The difference between the Fig. 3 and Fig. 10 is the resonance current path in the modes I and III. The input current is divided to the path through an upper arm (L_1, C_1, C_2) and the path through a lower arm (L_1, C_6, C_7). For this reason, the relationship between the circuit parameters and input impedance has changed. In this paper, the parasitic capacitances of the diodes are used as the capacitors C_1, C_2, C_6 and C_7. Thus, the resonance inductance is changed from 950 nH to 1.5 μH.

Fig. 11 presents the operation waveforms when the parasitic capacitance is used as a resonance capacitor. The DC output is obtained from an 13.56-MHz AC. Additionally, it is clarified that the sinusoidal input current and unity input power factor are obtained.

Fig. 12 shows the harmonic analysis results with the improved AC-DC converter. The input current total harmonic distortion (THD) of 8.1% is achieved with the bandwidth up to 20th. A THD with the improvement is suppressed by 27.7% compared with the one without improvement.

In addition, the input impedance is calculated

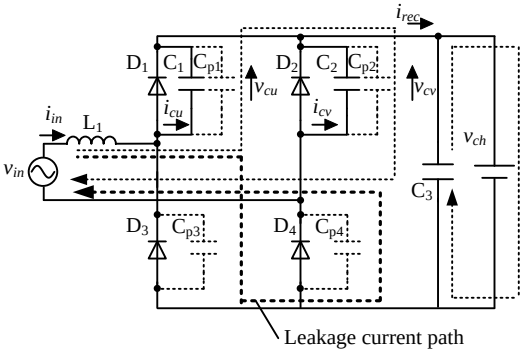

Fig. 8. Effect of the parasitic capacitances in the mode I.

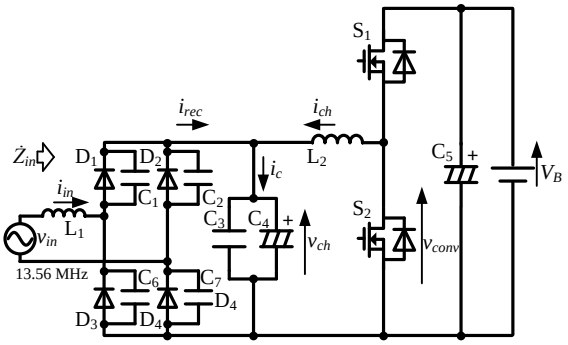

Fig. 9. Improved AC-DC converter with input impedance matching.

Table III: Parameters of the circuit components in the improved AC-DC converter.

Items		Manufactures	Model number	Value
MOSFET	S_1, S_2	Vishay	IRFB11N50APBF	500 V, 11 A
Diode	D_1-D_4	Cree	C3D08060A	600 V, 8 A
Inductor	L_1	TDK	VLF10040T-1R5N8R9	1.5 μH
	L_2	-	-	2.3 mH
Capacitor	$C_{1\text{-}2}$, $C_{6\text{-}7}$	-	(Parasitic capacitances of the diodes)	(34.3 pF)
	C_3	TDK	CKG57NX7R2J474M	470 nF (in parallel)
	C_4	nichicon	UPW2V221MRD	220 μF (in parallel)
	C_5	BHC Components	ALS30A221DB450	220 μF

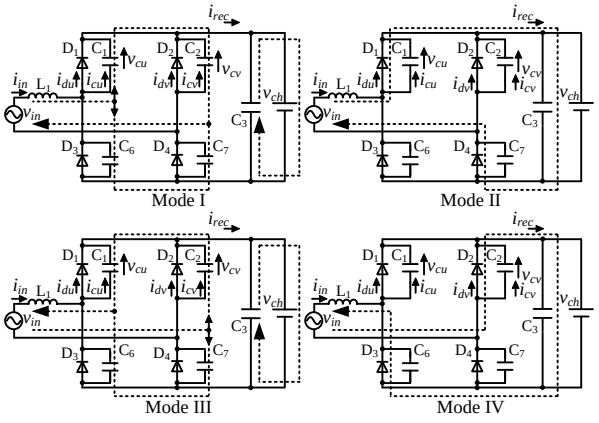

Fig. 10. Operation modes of the improved AC-DC converter.

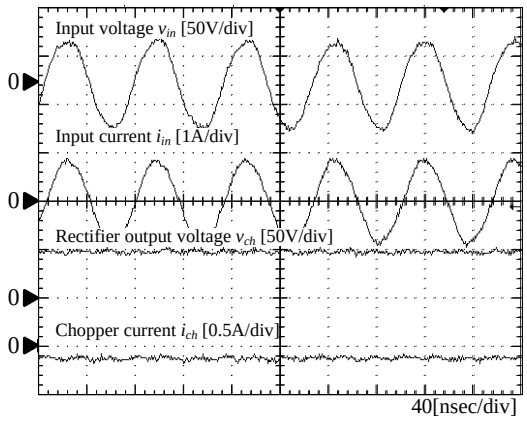

Fig. 11. Operation waveforms of the improved AC-DC converter.

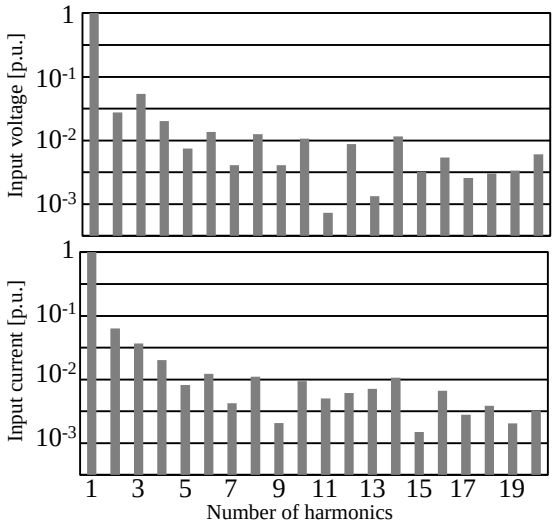

Fig. 12. Harmonics components of the input voltage and input current in the improved AC-DC converter.

as 52.7 - *j*0.02 Ω. The reflection coefficient, which is calculated by (9), is Γ = 2.6%. The reflection coefficient is used to evaluate a matching characteristic of the high-frequency circuit in the research field related to high-frequency circuit. If the impedance matching is completely held, the reflection coefficient is zero.

It means that the ratio of the reflected power which occurs at the input of the circuit to the travelling power is lesser than 0.1%. It is clarified that the proposed AC-DC converter suppresses the reflected power from the above experiments. Thus, the proposed circuit can be applied to the receiving side of the wireless power transfer system.

5.3. Comparison of the reflection coefficient

In this subsection, the reflection coefficients are compared among the conventional CI-DBR, proposed converter without the improvement and the proposed converter with the improvement.

Generally, the input impedance matching of the CI-DBR is not achieved in the reason of the distorted input current and low input power factor. Moreover, the reflection coefficient of the conventional CI-DBR depends on the load conditions and a smoothing capacitor widely. In contrast, the reflection coefficient of the proposed circuit does not depend on the load condition and a value of the smoothing capacitor.

Fig. 13 shows the comparison result of the reflection coefficient which is calculated from (10) among the conventional CI-DBR and the proposed AC-DC converters. Note that the conventional CI-DBR has a smoothing capacitor of 0.47 μF. The proposed converter with the improvement and one without the improvement achieve the input impedance matching with the reflection coefficients of 2.6% and 29.3% respectively. It is clear that the reflection coefficient can be suppressed compared to the conventional CI-DBR. In particular, the reflection coefficient with the improved AC-DC converter suppresses the reflection coefficient by 94.5 % compared with the conventional CI-DBR with a load of 25 Ω.

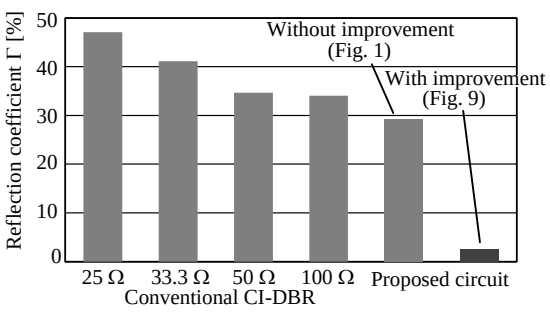

Fig. 13. Comparison of the reflection coefficient between the conventional CI-DBR and proposed circuit.

VI. Conclusion

This paper discussed the AC-DC converter which converts power from 13.56-MHz AC to DC for a receiving side of a wireless power transfer system with a sinusoidal input current. The wireless power transfer systems are required

to operate in high-frequency such as 13.56 MHz in order to achieve a high power density of transmitting coils. Thus, the AC-DC converter in the receiving side is required to operate at high-frequency. In such high-frequency region, the reflected power occurs when the input impedance is not matched to the characteristic impedance of the transmission line. In other words, the input impedance of the AC-DC converter needs to have the same impedance to the characteristic impedance of transmission lines.

In order to overcome the above-mentioned problem, two AC-DC converters are proposed and experimentally tested. The both AC-DC converters achieve the input impedance matching without high-frequency switching devices except the diodes with a simple configuration. The experimental results confirmed that the proposed converter with the improvement enable a conversion from 13.56-MHz AC to DC with the sinusoidal input current. From the experimental results, one of the proposed converters has an error on the real part of the input impedance. In order to improve this problem, the second converter is proposed. The proposed converter has two additional capacitors compared to the AC-DC converter without the improvement. The experimental results confirmed that the input impedance of 52.7 - j0.02 Ω is achieved. It means that the reflection coefficient is suppressed by up to 94.5 % in comparison with the conventional diode bridge rectifier with a load of 25 Ω.

References

[1] J. J. Casanova, Z. N. Low, J. Lin: "A Loosely Coupled Planar Wireless Power System for Multiple Receivers", *IEEE Trans. On Industrial Electronics*, Vol. 56, No. 8, pp. 3060-3068 (2009)

[2] S. A. Adnan, M. Amin, F. Kamran: "Wireless power transfer using microwaves at 2.45 GHz ISM band", *IBCAST 2009*, pp. 99-102 (2009)

[3] A. Karalis, J. D. Joannopoulos, M. Soljacic: "Efficient Wireless non-radiative mid-range energy transfer", *Annals of Physics*, Vol. 323, No. 1, pp. 34-48 (2008)

[4] A. Kurs, A. Karalis, R. Moffatt, J. D. Joannopoulos, P. Fisher, M. Soljacic: "Wireless Power Transfer via Strongly Coupled Magnetic Resonances", *Science*, Vol. 317, pp. 83-86 (2007)

[5] S. Lee, R. D. Lorenz: "Development and Validation of Model for 95%-Efficiency 200-W Wireless Power Transfer Over a 30-cm Air-gap", *IEEE Trans. On Industry Applications*, Vol. 47, No. 6, pp. 2495-2504 (2011)

[6] Y. Suh, K. Chang: "A High-Efficiency Dual-Frequency Rectenna for 2.45- and 5.8-GHz Wireless Power Transmission", IEEE Trans. On Microwave Theory and Techniques, Vol. 50, No. 7, pp. 1784-1789 (2002)

[7] L. Chen, S. Liu, Y. C. Zhou, T. J. Cui: "An Optimizable Circuit Structure for High-Efficiency Wireless Power Transfer", *IEEE Trans. On Industrial Electronics*, Vol. 60, No. 1, pp. 339-349 (2013)

[8] A. P. Sample, D. A. Meyer, J. R. Smith: "Analysis, Experimental results, and Range Adaptation of Magnetically Coupled Resonators for Wireless Power Transfer", *IEEE Trans. On Industrial Electronics*, Vol. 58, No. 2, pp. 544-554 (2011)

[9] Y. Hori: "Future Vehicle Society based on Electric Motor, Capacitor and Wireless Power Supply", *IPEC 2010*, pp. 2930-2934 (2010)

[10] S. Cheon, Y. Kim, S. Kang, M. L. Lee, J. Lee, T. Zyung: "Circuit-Model-Based Analysis of a Wireless Energy-Transfer System via Coupled Magnetic Resonances", *IEEE Trans. On Industrial Electronics*, Vol. 58, No. 7, pp. 2906-2914 (2011)

[11] J. R. Long: "Monolithic Transformers for Silicon RF IC Design", *IEEE Trans. On Solid-state Circuits*, Vol. 35, No. 9, pp. 1368-1382 (2000)

[12] K. Kusaka, J. Itoh: "Experimental Verification of Rectifiers with SiC/GaN for Wireless Power Transfer Using a Magnetic Resonance Coupling", *IEEE 9th PEDS*, pp. 1094-1099 (2011)

[13] B. Singh, B. N. Singh, A. Chandra, K. Al-Haddad, A. Pandey, D. P. Kothari: "A Review of Single-Phase Improved Power Quality AC-DC Converters", *IEEE Trans. On Industrial Electronics*, Vol. 50, No. 5, pp. 962-981 (2003)

[14] K. Matsui, I. Yamamoto, K. Ando, G. Erdong: "A Novel High DC Voltage Generator by LC Resonance in Supply Frequency", *EPE2007*, pp. 1-8 (2007)